Contents

S1. CPC FARM detection efficiency curves

Figure S1 displays the detection efficiency curves of each channel of the Condensation Particle Counters For Atmospheric Rapid Measurements (CPC FARM) for positively charged ammonium sulfate particles. To avoid electrometer noise, detection efficiency measurements were set to 0 where the measured electrometer concentration was less than 50 cm^{-3}. For almost all temperature settings, the detection efficiency reaches a plateau maximum which is not 100%. This is due to diffusional wall loss inside the CPC FARM. Note, the plateau in the detection efficiency was not reached when the conditioner and initiator temperatures were set to 5 and 35 °C, respectively (and subsequently noted as 5/35 °C), due to the maximum size range of the Half Mini DMA as configured. Figure S1 shows that the five channels behave similarly. The lowest d_{50} was found at the maximum difference between condition and initiator stages and ranged between 1.56 and 1.74 nm between the 5 channels. On all five channels, as the difference between the conditioner and initiator temperatures decreased, the d_{50} increased at a higher rate.

A fitted model, given in Eq. Eq. (S1), is shown as solid lines in Figure S1.

$$\eta(x) = \eta_{\max}\left[1 - \exp\left(-\ln(2)\left(\frac{x - d_0}{d_{50,\mathrm{cal}} - d_0}\right)\right)\right]\eta_{\mathrm{GK}}(x, L_{\mathrm{eff}}, q_{\mathrm{a}}) \qquad \text{Eq. (S1)}$$

x describes the particle diameter, η_{max} describes the maximum efficiency (plateau) at $x >> d_{50}$, d_0 describes the diameter where the detection efficiency begins to increase from 0%, $d_{50,cal}$ describes the diameter where the detection efficiency reaches 50% assuming no diffusion losses, and η_{GK} is the (size-dependent) particle transmission efficiency in laminar flow through a tube (Gormley and Kennedy, 1948) which is parameterized with an effective tube length (L_{eff}) for given aerosol flowrate (q_a). The parameters used in Eq. (S1) for each channel are summarized in Table S1. For the 5/35 °C curve, a point was artificially added at 100 nm at the max detection efficiency of the 1/41 °C conditioner/initiator settings for the curve fit. The 5/35 °C curve fit is for visual reference only and was not used to extrapolate setpoint temperatures.

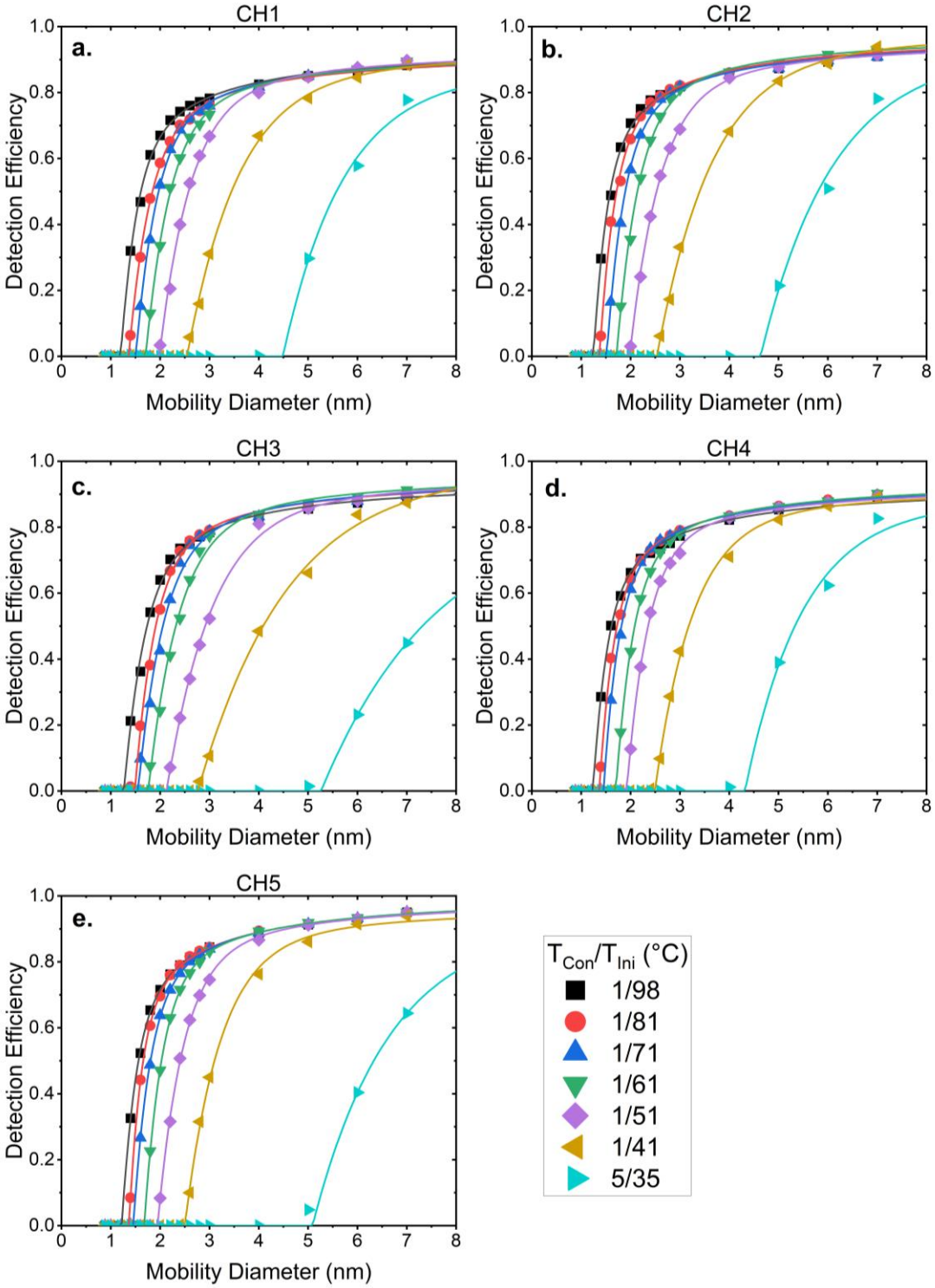

Figure S1. Detection efficiency curves for each of the five channels sorted by cut-point used during the Pittsburgh campaign with Channel 1 was set to the lowest cut-point. Each color/symbol represents a different set of conditioner and initiator temperatures. Solid lines represent the fitted model.

Table S1. CPC FARM fitted particle detection efficiency parameters

	η_{max}	d_0 (nm)	$d_{50,cal}$ (nm)	L_{eff} (m)	q_a (L min^{-1})
Ch. 1	0.934	1.201	1.378	0.050	0.300
Ch. 2	0.972	1.426	1.616	0.050	0.300
Ch. 3	0.958	1.604	1.913	0.050	0.300
Ch. 4	0.934	2.038	2.346	0.050	0.300
Ch. 5	0.979	2.421	2.851	0.050	0.300

S2. CPC FARM Live time fraction

Figure S2 shows the relationship between live time fraction, f_L, and the calculated number concentration reported by each channel, N_i, of the CPC FARM. The data shown were taken in Pittsburgh, PA between October 11th and 14th 2023. The live time fraction describes the amount of time within each CPC sampling interval where the detector can detect a particle. As the particle counts increase, the fraction live time decreases. The fraction of real particles detected by the CPC detector over the sampling interval decreases and a correction factor is needed to resolve the true particle concentration. A fitted model, given in Eq Eq. (S2), is shown as solid lines in Figure S2.

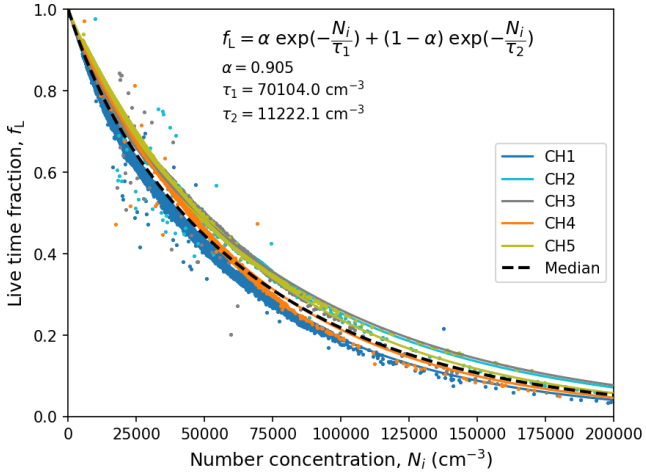

Figure S2: Plot showing the relationship between live time fraction and the calculated number concentration measured by each channel of the CPC FARM. Points represent the raw data points. Solid lines represent the curve fitted to the displayed equation. The constants are provided for the median fit. Data were taken between October 11th, 2023 and October 14th 2023.

$$f_L(N_i) = \alpha \exp\left(-\frac{N_i}{\tau_1}\right) + (1-\alpha)\exp\left(-\frac{N_i}{\tau_2}\right) \qquad \text{Eq. (S2)}$$

where N_i describes the number concentration, and α, τ_1 and τ_2 are fitting parameters. In the future, the live time fraction of the CPC-FARM could easily be increased by reducing the nozzle diameter.

S3. η_{max} variation over time

Figure S3 shows the η_{max} calculated daily over from June 15th, 2024 to June 28th, 2024. The study was conducted at the Department of Energy Atmospheric Radiation Measurement Southern Great Plains (SGP) field site in Billings, OK. The CPC FARM was set up as described in Fig. 1. The study was conducted at SGP because, unlike Pittsburgh in Fall 2023, there were weeks where each day had significant periods without sub-10 nm particles in the size distribution.

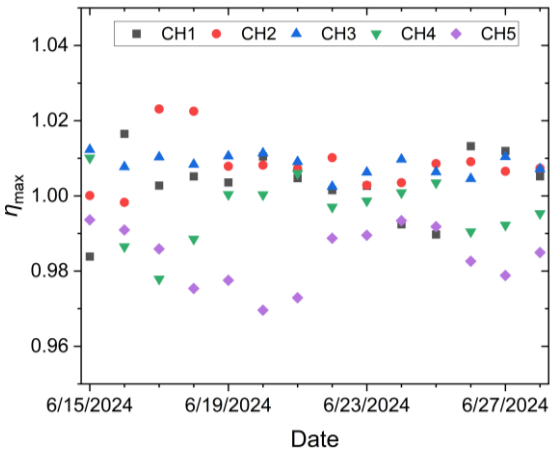

Figure S3: Plot showing the variation of η_{max} for the CPC FARM. Data were taken between June 15th, 2024 and June 28th, 2024 at the Department of Energy Atmospheric Radiation Measurement Southern Great Plains field site.

The η_{max} represents the overall transmission efficiency of each channel on the CPC FARM. The η_{max} was found by taking the ratio of N_i on each channel to the average of N_i across all channels over the 10-minute span where both ΔN and the change in sum of ΔN across all channels is the lowest. The plot shows that η_{max} only varies ±2% of the starting value within these two weeks and does not consistently drift over time.

S4. Simulated data inversion with low-concentration input

Figure S4 shows a simulated data inversion example similar to that shown in Fig. 5. The input distribution here has the same modal parameters as the original example, but the particle number in the <5 nm mode is reduced from 5,000 to 500 cm^{-3} to demonstrate the inversion performance and expected error at low differential signal levels. The numerical inversion still shows good agreement with the true input, and the approximate inversion is still lower than the true input.

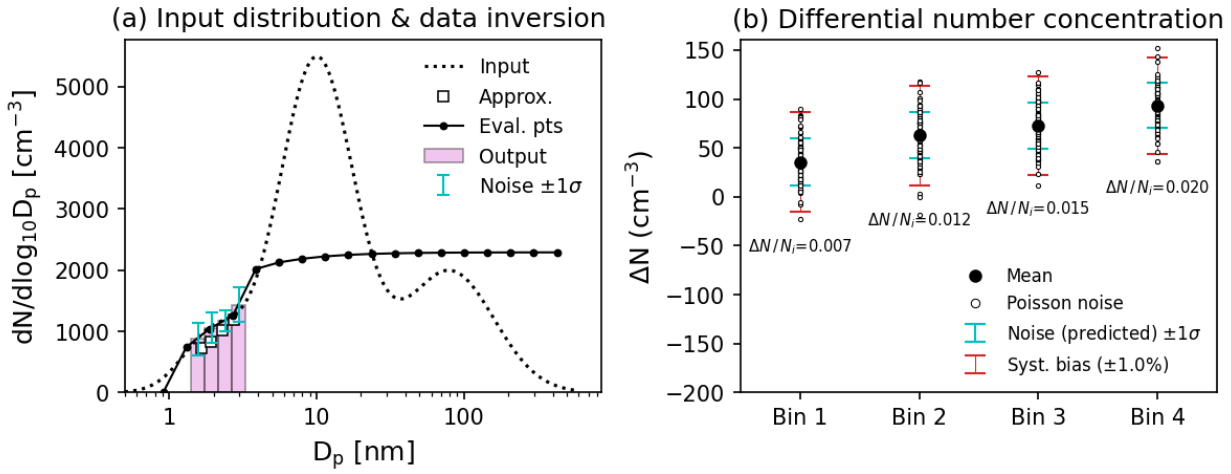

Figure S4. Simulated data inversion example with a 3-mode lognormal distribution. a) Output (numerical data inversion, bars) and approx. (approximate data inversion, square points) vs. input size distribution (dots) for noisy CPC FARM signals. Blue error bars represent 1σ of instrument noise. Black points are the 20 evaluation points used in the particle size vector for the kernel matrix Eq. (5). b) The resulting differential number across the instrument channels (mean values and noise due to random Poisson error), as well as systematic error due to ±1% bias in the signal of the first channel of each bin. ΔN/Nᵢ values indicate the relative differential number concentration in each bin. A sample flow rate of 0.3 L min^{-1} and a sampling time interval of 5 s were used in this example.

S5. CPC FARM approximate inversion compared to PSD

Figure S5 displays the particle size distribution measured in Pittsburgh on October 12th, 2023 by the CPC FARM inverted using the numerical and approximate methods. In the approximate inversion, the second and third largest size bins are lower and higher, respectively, compared to the numerical inversion. These discrepancies can be attributed to the incorrect assumption of step-function detection efficiency curves as the approximate inversion cannot account for overlap in the detection efficiency curves between neighboring channels nor the true shape of the sigmoidal detection efficiency curve.

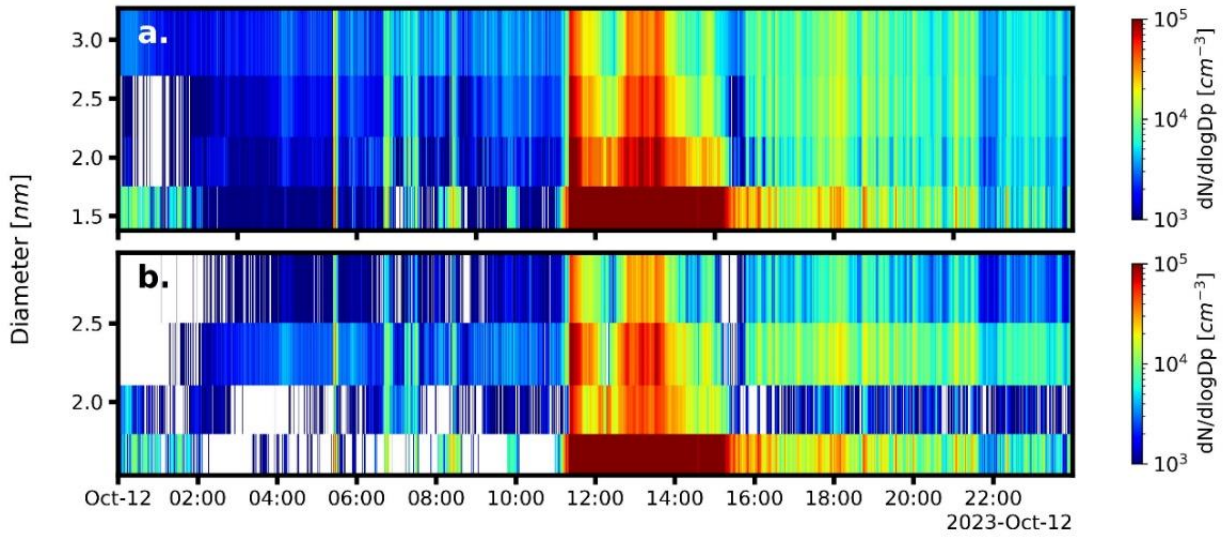

Figure S5: 1.6 – 2.9 nm size distributions taken on October 12th, 2023. (a) Contour plot showing the numerically inverted CPC FARM data recorded at 1 Hz with a 10-second average applied. The midpoints of the four size bins are 1.6, 1.9, 2.3, and 2.9 nm. (b) Contour plot showing the CPC FARM data inverted with the approximate method. The midpoints of the four size bins are 1.7, 1.9, 2.3, and 2.7 nm.

S6. Comparison of CPC FARM and PSD

Figure S6 shows parity plots of the PSD and CPC FARM at the midpoint of each size bin of the CPC FARM and the closest corresponding size bin midpoint of the PSD. For each data point, the CPC FARM observations were averaged over the five minutes of the corresponding PSD scan. The figure shows that at 1.6 and 1.9 nm, PSD measured concentration does not increase with increasing concentration measured by the CPC FARM. Between 2 and 3 nm, the PSD appears to undercount particle concentration by 50%. This figure also shows that the noise of the PSD decreases from 500,000 cm^{-3} to 20,000 cm^{-3} as the size increases from 1.6 to 2.4 nm. This is not surprising as the SMPS correction factors are larger for smaller sizes to due to lower charging efficiency and higher diffusion losses.

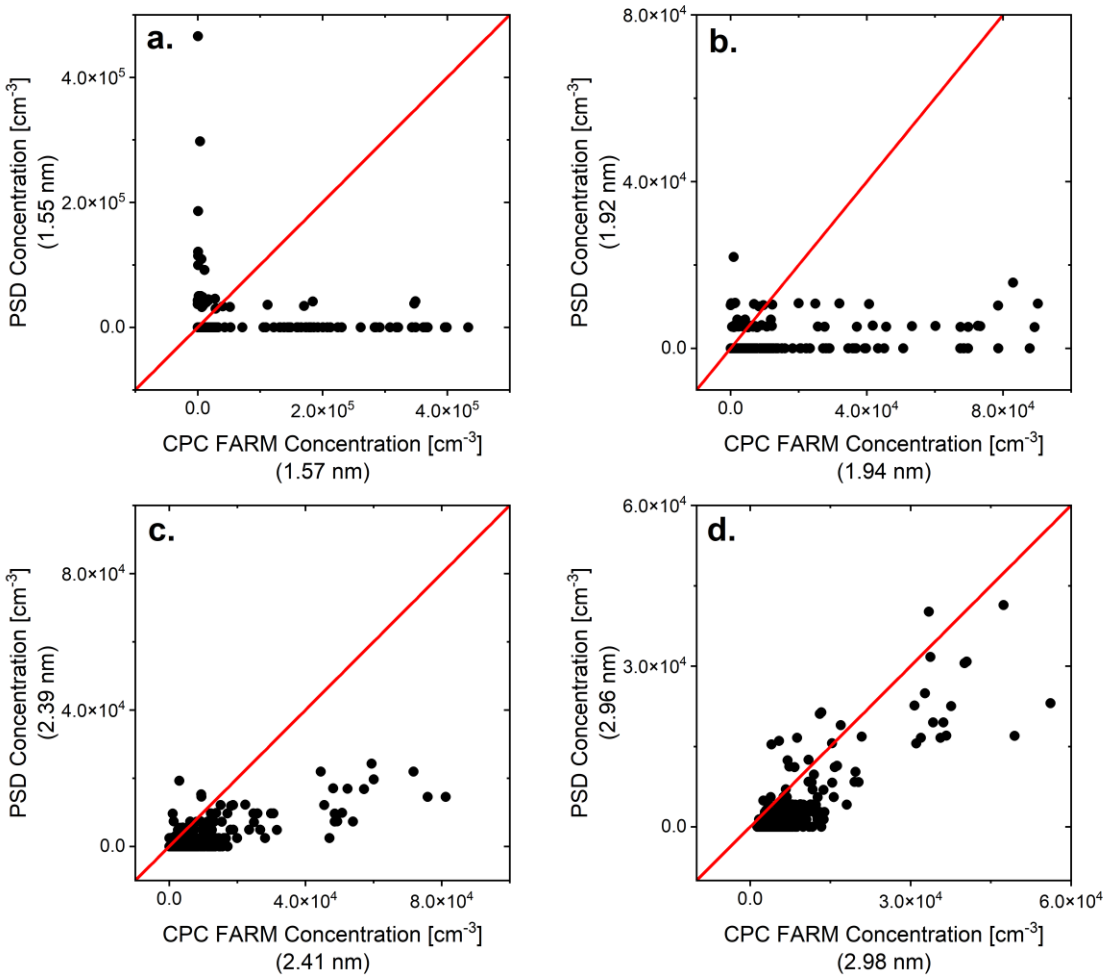

Figure S6 Parity plots comparing the PSD concentration at four size bins to their corresponding CPC FARM concentrations. The size-bin midpoints for each are displayed within the brackets. The solid red line is the parity line.

References

Riipinen, I., H. E. Manninen, T. Yli-Juuti, M. Boy, M. Sipilä, M. Ehn, H. Junninen, T. Petäjä, and M. Kulmala. 2009. “Applying the Condensation Particle Counter Battery (CPCB) to Study the Water-Affinity of Freshly-Formed 2–9 Nm Particles in Boreal Forest.” *Atmospheric Chemistry and Physics* 9 (10): 3317–30. https://doi.org/10.5194/acp-9-3317-2009.